ORIGINAL RESEARCH

Relationship between electronic structures and antiplasmodial activities of xanthone derivatives: a 2D-QSAR approach

Gaston A. Kpotin[1] · Affoué Lucie Bédé[2] · Alice Houngue-Kpota[1] · Wilfried Anatovi[1] · Urbain A. Kuevi[1] ·
Guy S. Atohoun[1] · Jean-Baptiste Mensah[1] · Juan S. Gómez-Jeria[3] · Michael Badawi[4]

Abstract

Malaria is an important disease causing many death in several countries of Africa and Asia. In these continents, some plants such as *Garcinia cola* are used to fight against this disease because they contain xanthone derivatives which present antiplasmodial activity. The present theoretical study aims to establish a relationship between the electronic structure and the antiplasmodial activity of some xanthone derivatives, and more specifically to build a 2D-pharmacophore model in order to predict the biological activity of xanthone derivatives. The calculations are performed within the density functional theory (DFT) using the B3LYP/6-31G(d,p) level of theory. The developed approach quantitative structure-activity relationship (QSAR) follows the Klopman-Peradejordi-Gómez (KPG) methodology. We obtain a statistically significant equation relating the variation of the logarithm of half maximal inhibitory concentration ($\log(IC_{50})$) with the variation of the numerical values of a set of eight local atomic reactivity descriptors ($R = 0.98$, $R^2 = 0.97$, adj-$R^2 = 0.95$, $F(8.13) = 48.63$, $p < 0.00000$, SD 0.08). The antiplasmodial activity seems to be driven by atomic orbitals and charges. Our 2D-pharmacophore model should be useful to propose new xanthone derivatives with higher antiplasmodial activity.

Keywords Xanthone · Antiplasmodial · QSAR · DFT · Klopman-Peradejordi-Gómez approach · Malaria

Introduction

Malaria is one of the most fatal diseases in the developing countries of Africa. In 2016, 91 countries reported a total of 216 million cases of malaria, an increase of 5 million cases over the previous year. The global tally of malaria deaths reached 445 000, about the same number reported in 2015 [1]. Malaria cases were caused by five types of parasite, being *Plasmodium falciparum*. Most of the treatments used to fight against *Plasmodium falciparum* include the artemisinin combinatory therapy (ACT). In fact, failures of the ACTs (artesunate/mefloquine and artesunate/amodiaquine) have recently been reported as frequent failures of dihydroartemisinin/piperaquine in parts of Cambodia, and decreasing sensitivity to lumefantrine may further threaten artemether/lumefantrine [2]. Likewise, some strains of *Plasmodium falciparum* such as FcB1 [2, 3], K1 W2, and TM4 strains are chloroquino-resistant [2–6]. Consequently, the development of new combinations of active compounds becomes crucial to fight against malaria disease.

In the last two decades, some research on xanthone derivatives as anti-malarial agents was published. Winter et al. have identified 2,3,4,5,6-pentahydroxyxanthone (X5) as a potent antimalarial drug with equal activity against multidrug-resistant strains of *P. falciparum* D6 clones [7]. Then, Ignatushchenko et al. have suggested that xanthones act in a unique way to kill *Plasmodium* through the formation of soluble complexes with heme, therefore inhibiting the process of heme polymerization [8, 9]. Hay et al. have

✉ Gaston A. Kpotin
  gaston.kpotin@fast.uac.bj

✉ Michael Badawi
  michael.badawi@univ-lorraine.fr

1   Laboratory of Theoretical Chemistry and Molecular Spectroscopy, Faculty of Sciences and Techniques, University of Abomey - Calavi, 03 BP 3409 Cotonou, Benin

2   Laboratoire de Chimie Organique Structurale, Université Félix Houphouët-Boigny, 22 BP 582, Abidjan, Côte d'Ivoire

3   Quantum Pharmacology Unit, Department of Chemistry, Faculty of Sciences, University of Chile, Las Palmeras 3425, Ñuñoa, 7800003 Santiago, Chile

4   Laboratoire de Physique et Chimie Théoriques, Université de Lorraine - CNRS, Nancy, France

isolated thirteen xanthones from *Garcinia vieillardii* and have synthetized nine others. They evaluated the antimalarial activity of these xanthones against chloroquino-resistant strains of *Plasmodium falciparum* FcB1/Colombia. The results showed that the position of the hydroxyl groups appears to be important as indicated by the differences of activities [10]. Concerning the activity of xanthones on *P. falciparum* K1 strain, Mahabusarakam et al. have shown that the best activity was achieved by addition of alkylamino or hydroxyalkylamino groups to either or both phenolic hydroxyl groups [11]. Upegui et al. have isolated α-mangostin and δ-mangostin (1,2,3,6,7-pentahydroxy-4,8 diisoprenylxanthone) from mangosteen husk. They observed that α-mangostin was more active against the resistant *P. falciparum* chloroquine-resistant (FCR3) strain (IC50 = 0.2 ± 0.01 μM) than δ-mangostin (IC50 = 121.2 ± 1.0 μM) [12]. In 2016, Auranwiwat et al. isolated and characterized some xanthones; the most active they obtained is 1,6,7-trihydroxy-6,6′-dimethyl-2H-pyrano(2′,3′:3,2)-5-(4-acetoxy-3-methylbut-2-enyl)-8-(4-hydroxy-3-methylbut-2-enyl)-xanthone (IC50 = 6.0 μM) on strain TM4 of *Plasmodium falciparum* and bannaxanthones I (IC$_{50}$ = 3.6 μM) on K1 of *Plasmodium falciparum* [6]. Despite these studies, a model needs to be developed to explain the measured IC$_{50}$ as well as to predict the biological activity of new compounds. Therefore, it is important to link the antiplasmodial activity of a selection of xanthone derivatives to molecular descriptors in order to propose new efficient compounds. An elegant approach to tackle this issue is to use advanced statistical analysis combined with advanced quantum chemical calculations.

Indeed, the study of the structure-activity relationships (SARs) is useful for the synthesis of new and more active molecules. There are several statistics-based SAR methods for carrying out such task [13–17]. The usual QSAR studies employ equation without any previous conceptual development. Many descriptors use in the equation come from different realms: classical chemistry (solubility, ionization constants, experimental dipole moments, etc.), quantum chemistry (calculated dipole moments, atomic net charges, reactivity indices, etc.), 2D or 3D geometry, graph theory, etc. When several of these indices coming from different realms are mixed in the equation and a solution satisfying all confidence tests is obtained, the problem of the physical interpretation appears due to the empirical character of the equation. In the present study, we use the Klopman-Peradejordi-Gómez (KPG) approach, which is on the side of the model-based methods [18]. The equation obtained in this approach is the algebraic form of the hypothesis contained in the model. The KPG approach has proven to be very useful to disclose the relationships between electronic structure and biological activities [19–23]. One of the best proofs that the KPG method is superior to empirical methods is the prediction of the human dose of the DON hallucinogen and the suggestion of a molecule with stronger cannabinoid activity [22, 23].

In this paper, we present the results of a quantum-chemical analysis of the relationships between the electronic structure and the antiplasmodial activities of xanthone derivatives against *Plasmodium falciparum* strain FcB1. From the results obtained, we propose the associated two-dimensional (2D) antiplasmodial partial pharmacophores.

Methods, models, and calculations

Model and selection of molecules

Model

As the Klopman-Peradejordi-Gómez is in use after 25 years, we refer the reader to the references about the model itself [24–30] and its successful applications [22, 29, 31–33]. In summary, a biological activity BA for a given molecule can be represented by the following linear equation:

$$\log(BA) = a + bM_{D_i} + c\log\left[\sigma_{D_i}/(ABC)^{1/2}\right] + \sum_j \left[e_j Q_j + f_j S_j^E + s_j S_j^N\right] + \sum_j \sum_m \left[h_j(m)F_j(m) + x_j(m)S_j^E(m)\right]$$

$$+ +\sum_j \sum_{m'} \left[r_j\left(m'\right)F_j\left(m'\right) + t_j\left(m'\right)S_j^N\left(m'\right)\right] + \sum_j \left[g_j\mu_j + k_j\eta_j + o_j\omega_j + z_j\varsigma_j + w_j Q_j^{\max}\right] \tag{1}$$

where a, b, c, e_j, f_j, s_j, $h_j(m)$, $x_j(m)$, $r_j(m')$, $t_j(m')$, g_j, k_j, o_j, z_j, and w_j are constants, M_{D_i} is the drug's mass, σ_{D_i} is its symmetry number, ABC is the product of the drug's moments of inertia about the three principal axes of rotation, Q_j is the net charge of atom j, S_j^E and S_j^N are, respectively, the total atomic electrophilic and nucleophilic superdelocalizabilities of atom j, $F_{j,m}$ is the electron population (Fukui index) of the occupied (vacant) MO m(m′) localized on atom j, $S_j^E(m)$ is the atomic electrophilic superdelocalizability of MO m localized on atom j, μ_j is the local atomic electronic chemical potential of atom j, η_j is the local atomic hardness of atom j, ω_j is the local atomic electrophilicity of atom j, ς_j is the local atomic softness of atom

j, Q_j^{max} is the maximum amount of electronic charge that atom j may accept from another site, and O_k is the orientational parameters of the kth substituent.

Throughout this paper, $HOMO_j^*$ refers to the highest occupied molecular orbital localized on atom j ("local HOMO*") and $LUMO_j^*$ to the lowest empty MO localized on atom j ("local LUMO"). The new local atomic reactivity indices of Eq. 1 were derived within the Hartree-Fock-Roothan method and are defined as follows [24]. The descriptors are not normalized because they have a concrete physical meaning and units. Therefore, the coefficients are not normalized. This is necessary for keeping the physics of the equation and also to allow the comparison with other studies carried out with different molecules but owing the same receptors.

The local atomic electronic chemical potential is defined as follows:

$$\mu_i = \left(\varepsilon_{HOMO*,i} + \varepsilon_{LUMO*,i}\right)/2 \tag{2}$$

and represents the measure of the propensity of atom i to gain or lose electrons.

The local atomic hardness is defined as follows:

$$\eta_i = \left(\varepsilon_{HOMO*,i} - \varepsilon_{LUMO*,i}\right) \tag{3}$$

This index measures the resistance of atom i to exchange electrons with a site.

The local electrophilic superdelocalizability of the HOMO* of atom i:

$$S_i^{E*} = \frac{F_{i,HOMO*}}{\varepsilon_{HOMO*}} \tag{4}$$

The physical meaning of this index is the electron-donating capacity of atom i at occupied MO m.

The local nucleophilic superdelocalizability of the LUMO* of atom i:

$$S_i^{N*} = \frac{F_{i,LUMO*}}{\varepsilon_{LUMO*}} \tag{5}$$

It is a measure of the electron-accepting capacity of atom i at empty MO m′.

The local atomic softness of atom i is defined as:

$$s_i = \frac{1}{\eta_i} \tag{6}$$

This index is the inverse of the hardness, so it measures the facility of atom i to exchange electrons with the site.

Local atomic electrophilicity of atom i is defined as:

$$\omega_i = \frac{\mu_i^2}{2\eta_i} \tag{7}$$

This index measures the propensity of atom i to receive extra electronic charge together with its resistance to exchange charge with a site.

The maximal amount of which charge atom i may receive is defined as:

$$Q_i^{max} = -\frac{\mu_i}{\eta_i} \tag{8}$$

From a conceptual perspective, the work presented here is a test of the hypothesis stating that the KPG model can provide a quantitative and formal relationship between the molecular structure and any biological activity. Nowadays, the KPG model produced excellent results in all its applications [21, 29, 32, 33].

Selection of molecules

Molecules were selected from a set reported in the literature [10]. The molecules are shown in Fig. 1 and Table 1. Figure 2 shows the numbering of atoms used in the linear multiple regression analysis (LMRA). The experimental data employed in this study are in vitro antiplasmodial activity on *Plasmodium falciparum* strain FcB1/Colombia quantified as IC_{50} [10].

Calculations

The electronic structure of the molecules was obtained within the density functional theory (DFT) at the B3LYP/6-31G(d,p) level of theory with full geometry optimization. The Gaussian collection of programs was employed [34]. The local atomic reactivity indices were calculated from the single point log file with the D-Cent-QSAR software [35] with correction of the anomalous electron populations that sometimes are produced by the Mulliken population analysis [36]. All electron populations smaller than or equal to 0.01 e were considered as zero [36]. We employed the common skeleton hypothesis defined as a particular set of atoms, common to all molecules analyzed, that accounts for nearly all the biological activity. The variation of the values of a set of local atomic reactivity indices of one or more atoms belonging to this skeleton gives an account of the variation of the antiplasmodial activity
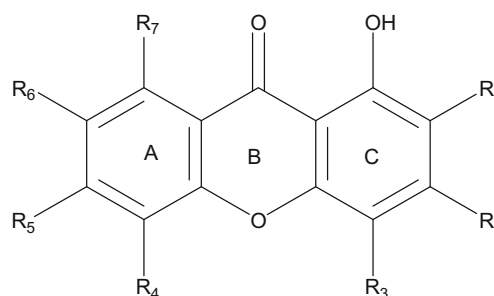

Fig. 1 Structure of xanthone derivatives

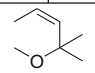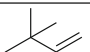**Table 1** Selected molecules and their antiplasmodial activities

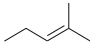| Mol	R_1	R_2	R_3	R_4	R_5	R_6	R_7	$\log(IC_{50})$
1	O in R_2			OH	H	H	H	0.54
2	O in R_2			H	H	OH		0.30
3	O in R_2		H	H	H	OH		0.42
4		OH	H	H	H	O in R_6		0.85
5	H	OH	H	H	H	O in R_6		1.07
6	O in R_2			OH	OH	H	H	0.68
7		OH	H	H	H	OH		0.32
8	H	H	H	H	OH	H	H	1.27
9	H	OH		OH	H	H	H	0.71
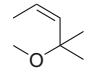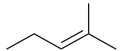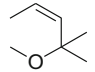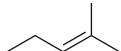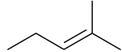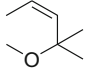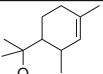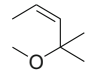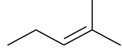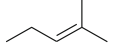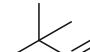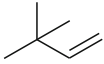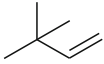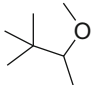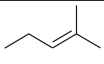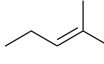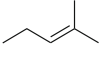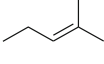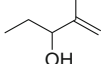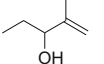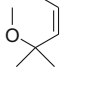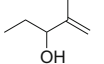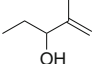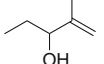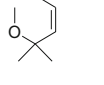
Table 1 (continued)

Mol	R$_1$	R$_2$	R$_3$	R$_4$	R$_5$	R$_6$	R$_7$	log(IC$_{50}$)
10	H	OMe	(structure)	OH	OH	H	H	0.97
11	H	OH	(structure)	OH	OH	H	H	0.85
12	H	(structure) O in R$_2$		OH	OH	H	H	1.03
13	H	H	OH	OH	H	H	H	1.16
14	H	OH	H	OH	H	H	H	2.01
15	(structure)	OH	H	OH	H	H	H	1.20
16	(structure)	OH	(structure)	OH	H	H	H	0.68
17	H	OH	(structure)	OH	H	H	H	1.12
18	(structure) OH	OH	H	OH	H	H	H	1.05
19	H	OH	(structure) OH	OH	H	H	H	1.30
20	H	(structure) O in R$_2$		OH	H	H	H	0.65
21	(structure) OH	OH	(structure) OH	OH	H	H	H	1.56
22	(structure) OH	(structure) O in R$_2$		OH	H	H	H	1.14

throughout the series analyzed. The common skeleton numbering is shown in Fig. 2.

We made use of linear multiple regression analysis (LMRA) using the Statistica software [37] to determine which atoms are directly involved in the variation of the biological activity. We built a matrix containing the dependent variable ($\log (IC_{50})$), and the local atomic reactivity indices of all atoms of the common skeleton as independent variables.

Results

The best statistically significant equation obtained is the following:

$$\log(IC_{50}) = 9.45 - 1.97\mu_6 - 1.84 S_{15}^N(LUMO)^* - 17.61 S_{16}^E(HOMO)^*$$
$$- 20.18 F_{16}(HOMO-2)^* - 50.56 Q_{16} - 0.81 F_5(LUMO+1)^* \quad (9)$$
$$+ 0.14 S_8^E(HOMO-2)^* + 0.07 S_{16}^N(LUMO+1)^*$$

with $n = 22$, $R = 0.99$, $R^2 = 0.98$, adj-$R^2 = 0.97$, $F(8.13) = 81.33$, $p < 0.000001$, and a standard error estimate of 0.07. No outliers were detected and no residual fall outside the $\pm 2\sigma$ limits. Here, μ_6 is the local atomic electronic chemical potential of atom 6, S_{15}^N $(LUMO)^*$ is the atomic nucleophilic superdelocalizability of the lowest empty MO localized on atom 15, $S_{16}^E(HOMO)^*$ is the atomic electrophilic superdelocalizability of highest occupied MO localized on atom 16, $F_{16}(HOMO-2)^*$ is the Fukui index of the third highest occupied MO localized on atom 16, Q_{16} is the net charge of atom 16, $F_5(LUMO+1)^*$ is the Fukui index of the vacant second lowest empty MO localized on atom 5, S_8^E $(HOMO-2)^*$ is the atomic electrophilic superdelocalizability of the third highest occupied MO localized on atom 8, and S_{16}^N $(LUMO+1)^*$ is the atomic nucleophilic superdelocalizability of (LUMO+1)* on atom 16.

The KPG method uses a model-based equation and must have a solution by definition. We use statistics to search the best equation and not to check if there is one. KPG method has not the

obligation to perform the external and internal validations because of its mathematical formal structure. Table 2 shows the beta coefficients and the t test results for the significance of coefficients of Eq. 9. Table 3 shows the squared correlation coefficients for the variables appearing in Eq. 9.

Table 3 shows that the highest internal correlation is r^2 $(S_{15}^N(LUMO)^*, \mu_6) = 0.26$. Figure 3 shows the plot of observed values vs. calculated values of $\log(IC_{50})$. The associated statistical parameters of Eq. 9 show that this equation is statistically significant and that the variation of the numerical values of eight LARIs explains about 95% of the variation of the biological activity.

To be able to suggest the type of molecular interactions that involve atoms appearing in Eq. 9, we determine the nature of their three highest occupied and three lowest empty local molecular orbitals. Table 4 shows the local molecular orbitals of atoms 5, 6, 15, and 16 (see Fig. 3). Nomenclature: Molecule (HOMO)/(HOMO-2)* (HOMO-1)* (HOMO)* - (LUMO)* (LUMO+1)* (LUMO+2)*. The number corresponding of the HOMO of each molecule is in bracket, and for each atom, we have the third local HOMO* and the third local LUMO*.

The molecular orbitals of molecule 2 (one of the most active) are represented in Fig. 4. Note that this MO is localized only on some atoms.

Discussion

The beta values (Table 3) shows that the importance of variables decreases in the following order: $\mu_6 > S_{15}^N(LUMO)^*$ $\approx S_{16}^E(HOMO)^* \approx F_{16}(HOMO-2)^* > Q_{16} > F_5(LUMO+1)^* > S_8^E(HOMO-2)^* \approx S_{16}^N(LUMO+1)^*$. Table 3 indicates that $S_8^E(HOMO-2)^*$ and $S_{16}^N(LUMO+1)^*$ have a low significance since the associated p values are higher than 0.005. Therefore, we will discuss only the six others indices. The process seems to be orbital and charge-controlled because seven
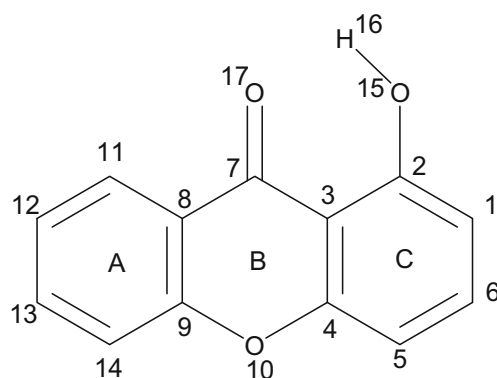
Fig. 2 Common skeleton of xanthone derivatives

Table 2 Beta coefficients and t test for significance of coefficients in Eq. 9

Variable	Beta	t (10)	p level
μ_6	− 0.90	− 18.52	< 0.000000
$S_{15}^N(LUMO)^*$	− 0.42	− 7.88	< 0.000003
$S_{16}^E(HOMO)^*$	− 0.41	− 9.43	< 0.000000
$F_{16}(HOMO-2)^*$	− 0.40	− 7.20	< 0.000007
Q_{16}	− 0.33	− 6.75	< 0.000014
$F_5(LUMO+1)^*$	− 0.19	− 3.68	< 0.003
$S_8^E(HOMO-2)^*$	0.14	3.05	< 0.009
$S_{16}^N(LUMO+1)^*$	0.12	3.02	< 0.010

Table 3 Squared correlation coefficients for the variables appearing in Eq. 9

	μ_6	$S_{15}^N(LUMO)^*$	$S_{16}^E(HOMO)^*$	$F_{16}(HOMO-2)^*$	Q_{16}	$F_5(LUMO+1)^*$	$S_8^E(HOMO-2)^*$
$S_{15}^N(LUMO)^*$	0.26						
$S_{16}^E(HOMO)^*$	0.01	0.08					
$F_{16}(HOMO-2)^*$	0.01	0.02	0.02				
Q_{16}	0.01	0.05	0.00	0.17			
$F_5(LUMO+1)^*$	0.00	0.07	0.08	0.23	0.01		
$S_8^E(HOMO-2)^*$	0.04	0.10	0.01	0.07	0.19	0.01	
$S_{16}^N(LUMO+1)^*$	0.01	0.00	0.00	0.08	0.00	0.00	0.01

indices depend on the electron population or/and the energies of the MOs and one depend on the net charge of atom 16.

For the discussion, we shall use the variable by variable (VbV) analysis. The local electronic chemical potentials are negative; the Fukui indices are always positive; the electrophilic superdelocalizabilities, total and partial, are negative; nucleophilic superdelocalizability is positive in general cases; and the charge of atom 16 is positive. So the VbV analysis shows that a good activity should be associated with low negative numerical values of μ_6 and $S_{16}^E(HOMO)^*$, high positive numerical values of $S_{15}^N(LUMO)^*$, $F_{16}(HOMO-2)^*$, Q_{16}, and $F_5(LUMO+1)^*$.

Let us now discuss these findings at the molecular scale.

Indeed, atom 6 is a carbon atom of the ring C (Fig. 2). The small negative value of μ_6 should be obtained by making less negative the HOMO* energy, making this atom a good electron donor. In Table 4, we observe two cases about the position of HOMO* and LUMO*. In the first case, the local HOMO* of atom 6 does not coincide with the molecular HOMO and the LUMO* coincides with the molecular LUMO (Table 4). In the second case, the local HOMO* of atom 6 coincides with the molecular HOMO and the LUMO* coincides with the molecular LUMO. In the first case, we have to make the HOMO* more reactive; in the second case, the LUMO* should be less reactive. Therefore, atom 6 seems to interact with an electron deficient center of a probable π nature.

Atom 15 is an oxygen atom of the hydroxyl group on the ring C (Fig. 2). The high positive value of $S_{15}^N(LUMO)^*$ should be obtained whether by raising the Fukui index of $LUMO_{15}^*$ or by lowering the $LUMO_{15}^*$ energy. In both cases, the $LUMO_{15}^*$ will be more reactive, so atom 15 interacts with an electron-rich center through its π empty orbitals.

Atom 16 is a hydrogen atom of the hydroxyl group on the ring C (Fig. 2). A good activity is associated with the low negative value of $S_{16}^E(HOMO)^*$ so the corresponding orbital should be less reactive and should be an inner MO. It is the case in all the molecules because $HOMO_{16}^*$ is energetically far from the molecular HOMO (Table 4). Atom 16 should interact with an electron-rich center. So atom 16 could participate to H-bond. This fact satisfies to the high value of Q_{16}. A high value of $F_{16}(HOMO-2)^*$ does not affect the value of $S_{16}^E(HOMO)^*$ and it would be obtained easily because we have the inner MO.

**Fig. 3** Plot of predicted vs. observed log(IC$_{50}$) values. Dashed lines denote the 95% confidence interval
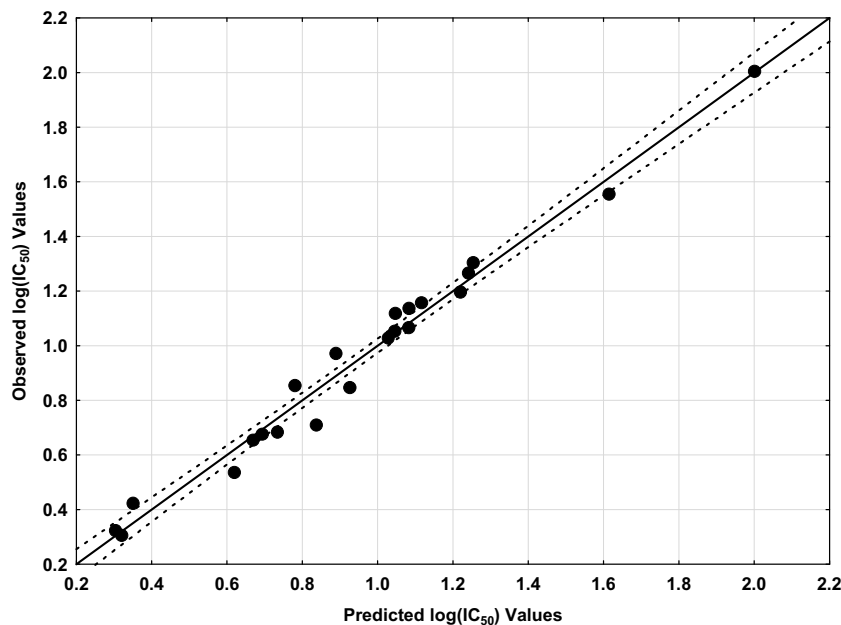
Table 4 Local molecular orbitals of atoms 5, 6, 15, and 16

Mol.	Atom 5 (C)	Atom 6 (C)	Atom 15 (O)	Atom 16 (H)
1 (100)	96π99π100π-101π102π103π	93π98π99π-101π102π103π	98π99π100π-101π102π103π	80σ82σ85σ-102σ103σ105σ
2 (119)	116π117π119π-120π121π122π	111π116π117π-120π121π122π	117π118π119π-120π121π122π	94σ100σ102σ-121σ123σ124σ
3 (100)	98π99π100π-102π103π104π	98π99π100π-101π102π103π	97π98π100π-101π102π103π	85σ88σ96σ-113σ114σ115σ
4 (100)	98π99π100π-101π102π103π	94π97π99π-101π102π103π	98π99π100π-101π102π104π	87σ89σ95σ-104σ108σ109σ
5 (100)	97π99π100π-101π102π103π	96π97π99π-101π102π103π	98π99π100π-101π103π104π	80σ83σ84σ-106σ107σ110σ
6 (104)	102π103π104π-106π108π109π	102π103π104π-105π106π107π	102π103π104π-105π106π108π	87σ90σ99π-118σ121σ123σ
7 (101)	99π100π101π-102π103π104π	94π97π98π-102π103π104π	98π99π101π-102π104π105π	86σ95σ96σ-105σ108σ110σ
8 (59)	56π57π59π-60π61π62π	55π56π59π-60π61π62π	56π57π59π-60π63π70π	46σ50σ51σ-65σ67σ68σ
9 (82)	79π81π82π-83π84π85π	79π81π82π-83π84π85π	80π81π82π-83π86π87π	66σ69σ70σ-89σ90σ92σ
10 (90)	88π89π90π-91π92π93π	87π89π90π-91π92π93π	88π89π90π-91π93π94π	71σ74σ79σ-97σ98σ99σ
11 (86)	84π85π86π-87π88π89π	83π85π86π-87π88π89π	84π85π86lp-87π90π96π	68σ71σ75σ-91σ93σ94σ
12 (86)	82π85π86π-87π88π89π	84π85π86π-87π88π89π	83π84π86π-87π90π97π	71σ73σ74σ-92σ93σ96σ
13 (63)	58π62π63π-64π65π66π	60π62π63π-64π65π66π	60π62π63π-64π67π74π	51σ54σ55σ-69σ70σ72σ
14 (63)	59π62π63π-64π65π66π	59π60π62π-64π65π66π	61π62π63π-64π66π67π	51σ52σ54σ-68σ69σ70σ
15 (82)	80π81π82π-83π84π86π	79π80π81π-83π84π86π	80π81π82π-83π85π86π	71σ74π77σ-85σ89σ90σ
16 (101)	95π100π101π-102π103π104π	97π98π100π-102π103π104π	99π100π101π-102π104π105π	92σ96σ97σ-105σ109σ110σ
17 (82)	80π81π82π-83π84π85π	80π81π82π-83π84π85π	80π81π82π-83π85π86π	64σ65σ70σ-88σ89σ90σ
18 (86)	84π85π86π-87π88π90π	83π84π85π-87π88π90π	81π85π86π-87π89π90π	75σ77σ78σ-89σ94σ98σ
19 (86)	83π85π86π-87π88π89π	83π85π86π-87π88π89π	84π85π86π-87π89π90π	71σ73σ74σ-94σ95σ96σ
20 (81)	76π80π81π-82π83π86π	78π80π81π-82π83π84π	78π79π81π-82π83π84π	66σ67σ69σ-87σ88σ89σ
21 (109)	107π108π109π-111π112π113π	106π107π108π-110π111π112π	104π108π109π-110π112π113π	88σ89σ103σ-121σ123σ124σ
22 (104)	98π103π104π-105π106π110π	101π103π104π-105π106π107π	101π102π104π-105π106π107π	90σ93σ94σ-110σ111σ113σ

Atom 5 is a carbon of ring C (Fig. 2). The fact that $(LUMO+1)_5^*$ appears in the equation indicates that $LUMO_5^*$ is also participating to the process. All the three

lowest vacant orbitals localized on atom 5 are π nature (Table 4). The high value of $F_5(LUMO+1)^*$ indicates that atom 5 should interact with electron-rich center; this interaction could be π-π or π-σ kind.

All these suggestions are presented in the partial 2D inhibition pharmacophore of Fig. 5.
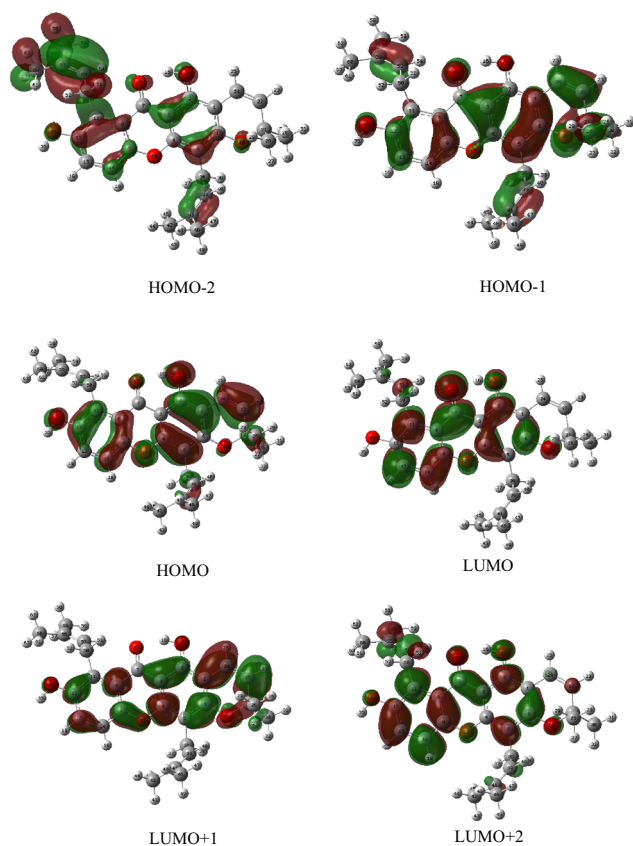
Fig. 4 Molecular orbitals of molecule 2

Conclusions

We obtained a statistically significant relationship between the variation of the antiplasmodial activities of some xanthones derivatives and the variation of the numerical values of a set of local atomic reactivity indices. This allowed us to build the
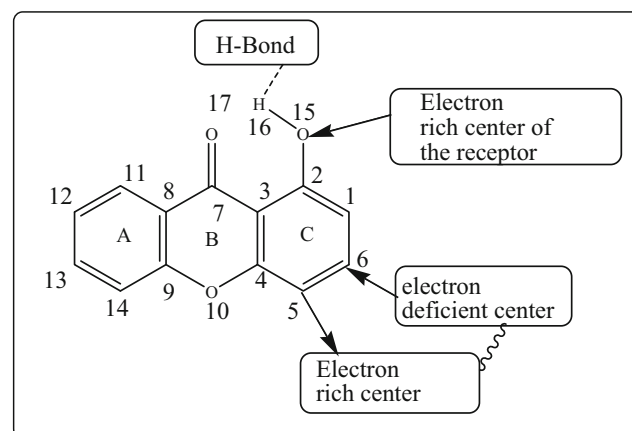
Fig. 5 Partial 2D pharmacophore for the antiplasmodial activities of xanthone derivatives on *Plasmodium falciparum* strain FcB1

associated pharmacophore that should serve as a starting point for chemical modifications producing more active compounds. The 2D-pharmacophore shows that the substitution on one ring can improve the antiplasmodial activity, and the presence of hydroxyl group near the carbonyl group plays an important function.

Compliance with ethical standards

Conflict of interest The authors declare that they have no conflict of interest.

References

1. World Health Organization and Global Malaria Programme World malaria report 2017 (2017) https://www.who.int/malaria/publications/worldmalaria-report-2017/en/. Accessed 29 Nov 2017
2. Rosenthal PJ, Rathod PK, Ndiaye D, Mharakurwa S, Cui L (2015) Antimalarial drug resistance: literature review and activities and findings of the ICEMR network. Am. J. Trop. Med. Hyg. 93:57–68
3. Menard D, Dondorp A (2017) Antimalarial drug resistance: a threat to malaria elimination. Cold Spring Harb. Perspect. Med. 7: a025619
4. Boudhar A, Ng XW, Loh CY, Chia WN, Tan ZM, Nosten F, Dymock BW, Tan KSW (2016) Overcoming chloroquine resistance in malaria: design, synthesis and structure–activity relationships of novel chemoreversal agents. Eur. J. Med. Chem. 119:231–249
5. Kalaria PN, Karad SC, Raval DK (2018) A review on diverse heterocyclic compounds as the privileged scaffolds in antimalarial drug discovery. Eur. J. Med. Chem. 158:917–936
6. Auranwiwat C, Laphookhieo S, Rattanajak R, Kamchonwongpaisan S, Pyne SG, Ritthiwigrom T (2016) Antimalarial polyoxygenated and prenylated xanthones from the leaves and branches of Garcinia mckeaniana. Tetrahedron 72:6837–6842
7. Winter RW, Cornell KA, Johnson LL, Ignatushchenko M, Hinrichs DJ, Riscoe MK (1996) Potentiation of the antimalarial agent rufigallol. Antimicrob. Agents Chemother. 40:1408–1411
8. Ignatushchenko MV, Winter RW, Bächinger HP, Hinrichs DJ, Riscoe MK (1997) Xanthones as antimalarial agents; studies of a possible mode of action. FEBS Lett. 409:67–73
9. Ignatushchenko MV, Winter RW, Riscoe M (2000) Xanthones as antimalarial agents: stage specificity. Am. J. Trop. Med. Hyg. 62: 77–81
10. Hay A-E, Hélesbeux J-J, Duval O, Labaïed M, Grellier P, Richomme P (2004) Antimalarial xanthones from Calophyllum caledonicum and Garcinia vieillardii. Life Sci. 75:3077–3085
11. Mahabusarakam W, Kuaha K, Wilairat P, Taylor W (2006) Prenylated xanthones as potential antiplasmodial substances. Planta Med. 72:912–916
12. Upegui Y, Robledo SM, Gil Romero JF, Quiñones W, Archbold R, Torres F, Escobar G, Nariño B, Echeverri F (2015) In vivo antimalarial activity of α-mangostin and the new xanthone δ-mangostin: antimalarial activity of a new xanthone. Phytother. Res. 29:1195–1201
13. Noguera GJ, Fabian LE, Lombardo E, Finkielsztein L (2015) QSAR study and conformational analysis of 4-arylthiazolylhydrazones derived from 1-indanones with anti-Trypanosoma cruzi activity. Eur. J. Pharm. Sci. 78:190–197
14. Shayanfar A, Shayanfar S (2014) Is regression through origin useful in external validation of QSAR models? Eur. J. Pharm. Sci. 59: 31–35
15. Shibi IG, Aswathy L, Jisha RS, Masand VH, Divyachandran A, Gajbhiye JM (2015) Molecular docking and QSAR analyses for understanding the antimalarial activity of some 7-substituted-4-aminoquinoline derivatives. Eur. J. Pharm. Sci. 77:9–23
16. Cheng Y, Luo F, Zeng Z, Wen L, Xiao Z, Bu H, Lv F, Xu Z, Lin Q (2015) DFT-based quantitative structure–activity relationship studies for antioxidant peptides. Struct. Chem. 26: 739–747
17. Toropov AA, Toropova AP, Benfenati E, Gini G, Fanelli R (2013) The definition of the molecular structure for potential anti-malaria agents by the Monte Carlo method. Struct. Chem. 24:1369–1381
18. Martin YC (1978) Quantitative drug design: a critical introduction Print book: English. Marcel Dekker, New York
19. Gomez-Jeria JS, Orellana Í (2016) A theoretical analysis of the inhibition of the VEGFR-2 vascular endothelial growth factor and the anti-proliferative activity against the HepG2 hepatocellular carcinoma cell line by a series of 1-(4-((2-oxoindolin-3-ylidene)amino)phenyl)-3-arylureas. Pharma Chem. 8:476–487
20. Gomez-Jeria JS, Valdebenito-Gamboa J (2015) A quantum-chemical analysis of the antiproliferative activity of N-3-benzimidazolephenylbisamide derivatives against MGC803, HT29, MKN45 and SW620 cancer cell lines. Pharma Chem. 7: 103–121
21. Robles-Navarro A, Gómez Jeria J (2016) A quantum-chemical analysis of the relationships between electronic structure and cytotoxicity, GyrB inhibition, DNA supercoiling inhibition and antitubercular activity of a series of quinoline–aminopiperidine hybrid analogues. Pharma Chem. 8:417–440
22. Gomez-Jeria JS, Cassels BK, Saavedra-Aguilar JC (1987) A quantum-chemical and experimental study of the hallucinogen (±)-1-(2,5-dimethoxy-4-nitrophenyl)-2-aminopropane (DON). Eur. J. Med. Chem. 22:433–437
23. GóMez-Jeria JS, Soto-Morales F, Rivas J, Sotomayor A (2008) A theoretical structure-affinity relationship study of some cannabinoid DERIVATIVES. J. Chil. Chem. Soc. 53
24. Gómez Jeria JS (2013) A new set of local reactivity indices within the Hartree-Fock-Roothaan and density functional theory frameworks. Can. Chem. Trans. 1:25–55
25. Gómez Jeria JS (2013) Elements of molecular electronic pharmacology1st edn. Ediciones Sokar, Santiago de Chile
26. Gómez Jeria JS (1982) Calculation of the nucleophilic superdelocalizability by the CNDO/2 method. J. Pharm. Sci. 71: 1423–1424
27. Gómez Jeria JS (1982) La Pharmacologie Quantique. Boll. Chim. Farm. 121:619–625
28. Gomez-Jeria JS (1983) On some problems in quantum pharmacology I. The partition functions. Int. J. Quantum Chem. 23:1969–1972
29. Gómez Jeria JS, Flores-Catalán M (2013) Quantum-chemical modeling of the relationships between molecular structure and in vitro multi-step, multimechanistic drug effects. HIV-1 replication inhibition and inhibition of cell proliferation as examples. Can. Chem. Trans. 1:215–237
30. Gómez-Jeria JS (1989) Modeling the drug-receptor interaction in quantum pharmacology. In: Maruani J (ed) Molecules in physics, chemistry, and biology. Springer Netherlands, Dordrecht, pp 215–231
31. Gomez-Jeria JS, Sotomayor P (1988) Quantum chemical study of electronic structure and receptor binding in opiates. J. Mol. Struct. THEOCHEM 166:493–498

32. Kpotin G, Atohoun SYG, Kuevi AU, Kpota-Hounguè A, Mensah J-B, Gómez Jeria JS (2016) A quantum-chemical study of the relationships between electronic structure and trypanocidal activity against *Trypanosoma brucei brucei* of a series of thiosemicarbazone derivatives. Pharm. Lett. 8:215–222

33. Gómez-Jeria JS, Cornejo-Martínez P (2016) A DFT study of the inhibition of human phosphodiesterases PDE3A and PDE3B by a group of 2-(4-(1H-tetrazol-5-yl)-1H-pyrazol-1-yl)- 4-(4-phenyl)thiazole derivatives. Pharma Chem. 8:329–337

34. Frisch MJ, Trucks GW, Schlegel HB, Scuseria GE, Robb MA, Cheeseman JR, Montgomery JA Jr, Vreven T, Kudin KN, Burant JC, Millam JM, Iyengar SS, Tomasi J, Barone V, Mennucci B, Cossi M, Scalmani G, Rega N, Petersson GA, Nakatsuji H, Hada M, Ehara M, Toyota K, Fukuda R, Hasegawa J, Ishida M, Nakajima T, Honda Y, Kitao O, Nakai H, Klene M, Li X, Knox JE, Hratchian HP, Cross JB, Adamo C, Jaramillo J, Gomperts R, Stratmann RE, Yazyev O, Austin AJ, Cammi R, Pomelli C, Ochterski JW, Ayala PY, Morokuma K, Voth GA, Salvador P, Dannenberg JJ, Zakrzewski VG, Dapprich S, Daniels AD, Strain MC, Farkas O, Malick DK, Rabuck AD, Raghavachari K, Foresman JB, Ortiz JV, Cui Q, Baboul AG, Clifford S, Cioslowski J, Stefanov BB, Liu G, Liashenko A, Piskorz P, Komaromi I, Martin RL, Fox DJ, Keith T, Al-Laham MA, Peng CY, Nanayakkara A, Challacombe M, Gill PMW, Johnson B, Chen W, Wong MW, Gonzalez C, Pople JA (2003) Gaussian 03, Revision B.04. Gaussian, Inc., Pittsburgh

35. Gómez-Jeria JS (2014) D-Cent-QSAR, a program to generate local atomic reactivity indices from Gaussian 03 log files. V.1.0, Santiago de Chile

36. Gómez-Jeria JS (2009) An empirical way to correct some drawbacks of Mulliken population analysis (Erratum in: J. Chil. Chem. Soc., 55, 4, IX, 2010). J. Chil. Chem. Soc. 54: 482–485

37. StatSoft, Inc. (2011) STATISTICA (data analysis software system), version 10. www.statsoft.com